Available online at www.sciencedirect.com

ScienceDirect

Procedia CIRP 31 (2015) 477 – 482

www.elsevier.com/locate/procedia

15th CIRP Conference on Modelling of Machining Operations

Enhanced Machinability of *Ti-5553* Alloy from Cryogenic Machining: Comparison with MQL and Flood-cooled Machining and Modeling

Y. Sun[a]*, B. Huang[a], D.A. Puleo[b], I.S. Jawahir[a]

[a]Department of Mechanical Engineering, and Institute for Sustainable Manufacturing (ISM), University of Kentucky, Lexington, KY 40506, USA
[b]Department of Biomedical Engineering, University of Kentucky, Lexington, KY 40506, USA
* Corresponding author. Tel.: +1 859 3233256; *E-mail address*: ying.sun@uky.edu

Abstract

Due to the high performance requirements such as high strength, excellent properties at room and high working temperatures, better resistance to corrosion and fatigue, etc., *Ti-5553* alloy has been generally considered as a suitable material to replace *Ti-6Al-4V* alloy in the aerospace industry for producing components, such as the advanced structural and landing gear. However, high chemical reactivity causing rapid tool-wear, low thermal conductivity resulting in high temperature and the formation of adiabatic shear bands introducing high dynamic loads and tool vibration during machining of *Ti-5553* alloy, have become the primary reasons limiting the application of this near beta-phase titanium alloy. This paper presents the results of a recent machinability study involving cutting forces, surface roughness and tool-wear aimed at improving the machinability of *Ti-5553* alloy by using cryogenic machining, and results are compared with those obtained from machining with flood cooling and minimum quantity lubrication (MQL) methods. Up to 30% reduction in the cutting forces could be achieved by cryogenic machining compared with flood cooling and MQL. MQL machining provides better surface roughness as higher ductility could be achieved due to the elevated temperatures. In the case of tool-wear, less nose wear is observed on the tool inserts used in cryogenic machining. Also, a finite element method (FEM) model is developed to simulate the cutting forces from cryogenic machining based on the modified Johnson-Cook flow stress model, and a good agreement is achieved between the experimental and predicted results.

Peer-review under responsibility of the International Scientific Committee of the "15th Conference on Modelling of Machining Operations

Keywords: Titanium alloy; Cryogenic machining;Cutting force; Tool wear; FEM.

1. Introduction

Cryogenic machining, with liquid nitrogen as the coolant, has been shown to be an effective method to significantly improve the surface integrity of manufactured components [1], in terms of surface and subsurface hardness, microstructure modification, phase transformation, residual stress, fatigue life etc. This surface integrity enhancement is often associated with improved machining performance, including the reduction of energy consumption (reducing cutting forces) and improved surface roughness, increased tool-life, the elimination of the conventional coolants etc. Kaynak et al. [2], in a recent study of cryogenic machining of *NiTi* alloy, showed increased microhardness in the machined subsurface. A similar observation was made by Rotella et al. [3] in the hardness profiles of the surface and subsurface in cryogenic machining of *Ti-6Al-4V* alloy. Pu et al. [4] showed the formation of a refined layer with nano-grains in cryogenic machining of *AZ31B Mg* alloy. Also, in another case, it was shown that the white layer thickness was limited on the machined surface of *AISI 52100* as a result of the lower temperature achieved by cryogenic cooling that restricted or prevented martensitic phase change [5]. Furthermore, more compressive residual stresses measured in the machined surface by Pusavec et al. [6] in cryogenic machining of Inconel *718* and by Outeiro et al. [7] in cryogenic machining of *AZ31B Mg* alloy, thus leading to improved fatigue life.

The three cutting force components were observed to be reduced in cryogenic machining of *NiTi* shape memory alloy compared with dry and preheating conditions [8]. Also, Kumar et al. [9] and Rotella et al. [10] reported similar trends in cryogenic machining of *Ti-6Al-4V* and *Al 7075* alloys in contrast to dry machining. Regarding tool-wear, both the notch wear and flank wear of the cutting tool inserts were significantly improved by cryogenic machining of *NiTi* alloy

Peer-review under responsibility of the International Scientific Committee of the "15th Conference on Modelling of Machining Operations
doi:10.1016/j.procir.2015.03.099

compared with dry and MQL-assisted machining [11]. Tool-life was improved by 1.28, 1.44 and 2.35 times in cryogenic machining of *Ti-6Al-4V* alloy when three different nozzle positions were used [12]. Improved surface roughness [13] and enhanced corrosion resistance [14] of *AZ31B Mg* alloy were also reported in cryogenic machining.

Due to the favorable mechanical properties, such as high strength and fracture toughness, low density, excellent resistance to fatigue and corrosion, *Ti-5553* alloy has been used in aerospace applications, including the advanced structural and landing gears [15-17], bulkhead components [18], nacelles, fuselages, wings and the corrosion prone areas difficult to inspect [19], in order to improve the durability of components and to optimize the weigh/resistance ratio. Also, a promising application in the military industry as the armor materials for armor-piercing projectiles has been shown [20].

However, *Ti-5553* alloy is one of the difficult-to-machine materials, whose machinability is very poor. Low cutting speeds have to be selected for prolonging the tool-life, thus the cycle time and manufacturing cost of machining is very high [15]. Compared to *Ti-6Al-4V* alloy, the specific mechanical properties of *Ti-5553* alloy, such as the higher hardness and tensile stress at elevated temperatures [21], make it very difficult to be machined. In addition, near-beta phase *Ti-5553* alloy with body centered cubic (BCC) structure is more stable than alpha-beta phase *Ti-6Al-4V* alloy with hexagonal close packed (HCP) structure. This is another primary reason for poor machinability of *Ti-5553* alloy.

Machining *Ti-5553* alloy draws great attentions from the research communities. The major research focus has been to reduce the cutting forces to limit the tool-wear. Baili et al. [15] used hot machining to heat the material before machining and maintain the desired temperature ranging from 100 to 800 ºC. They achieved 34% force reduction when the heating temperature was kept at 750 ºC. Although the tool-life was improved, it weakened the mechanical properties of *Ti-5553* alloy as the surface roughness and hardness were negatively influenced under certain machining conditions. The optimal machining parameters of *Ti-5553* alloy, including edge preparation (hone or chamfer), cutting speed, feed rate and tool rake angle, were determined by evaluating the related cutting forces, temperatures and tool-wear modes [22]. Machining of *Ti-5553* alloy with laser assistance was conducted by Braham-Bouchnak et al. [23], and a significant reduction of cutting forces was observed. However, the residual stresses became more tensile with laser power during machining that would weaken the fatigue life of the product.

In contract to hot or laser-assisted machining, cryogenic machining with liquid nitrogen as the coolant was used in this study of machining of *Ti-5553* alloy. Flood-cooled and MQL machining are also performed for comparison with cryogenic machining in terms of cutting forces and surface roughness. Tool-wear mechanism was analyzed by using the technology of energy-dispersive X-ray spectroscopy (EDX) associated with the optical images for measuring the crater and flank wear. Johnson-Cook material model was applied in the numerical model built based on the commercial FEM software DEFORM to simulate the cutting forces in dry and cryogenic conditions.

2. Experimental Work

The work material used in the machining experiments is *Ti-5553* (*Ti-5Al-5Mo-5V-3Cr*), in bar form with the diameter of 32 mm. Cutting speeds of 20, 50 and 80 m/min and the feed rates of 0.05, 0.125 and 0.2 mm/rev were used in the experimental work. A HAAS TL-2 CNC lathe was used for machining experiments with SANDVIK *432-MM* tool inserts with TiCN coating and 20 μm of cutting edge radius. Liquid nitrogen was delivered from the direction of the tool rake face with the flow rate of approximately *10g/s* mass under 1.5MPa pressure. A Kistler *9121* three-component tool dynamometer was used to measure the radial and tangential force components in flood-cooled, MQL and cryogenic machining.

Fig. 1 illustrates the experimental setup for cryogenic machining of *Ti-5553* alloy showing the details. The surface roughness of the machined samples was measured by a non-contact Zgyo NewView *5300* white light interferometer system. To observe and measure tool-wear, a Nikon EPIPHOT *300* with Leica DFC425 optical microscope was used, and the EDS measurement was conducted on a Hitachi *S-4300* system.

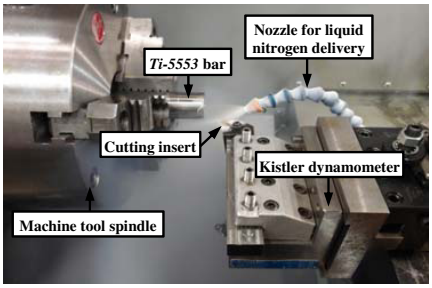

Fig. 1. Experimental setup for cryogenic machining *Ti-5553* alloy.

3. Results and Discussion

3.1. Tool-wear

Depending on the machining parameters, including cutting speed, feed rate, depth of cut, etc., and the work material and tool inserts, the commonly-known wear mechanisms are abrasive wear, adhesive wear, diffusion wear, microchipping, fatigue, delamination wear, etc. [24]. Based on the research of Wagner et al. [22], there exist two tool-wear modes in machining of *Ti-5553* alloys. The first tool-wear mode results from the abrasion process in machining, and the second wear mode is caused by a build-up edge. Nose and flank tool-wear of the inserts are shown in Fig. 2 for the conditions of flood-cooled, MQL and cryogenic machining of *Ti-5553* alloy when the cutting speed is 50 m/min and feed rate is 0.125 mm/rev. Observing from the tool-wear images, the abrasive flank wear is found in the nose areas for all the three machining conditions. Flank wear in the nose area is very similar and is insensitive to the cooling conditions as the mechanical properties of *Ti-5553* alloy are relatively stable due to its high strength, low ductility and high fracture toughness at room and elevated temperatures.

On the other hand, in order to identity the wear mechanism in the rake face of the inserts, EDS measurement was performed to test the compositions of the adhered material on the tool insert used in MQL machining at the cutting speed of 50 m/min and feed rate of 0.2 mm/rev. Fig. 3 shows the details of the images of the adhered material, the corresponding chemical compositions and their distributions. From those images, *Ti-5553* alloy was found to be present on the rake face of the tool insert, which indicates that adhesive wear was the primary mechanism of the nose wear.

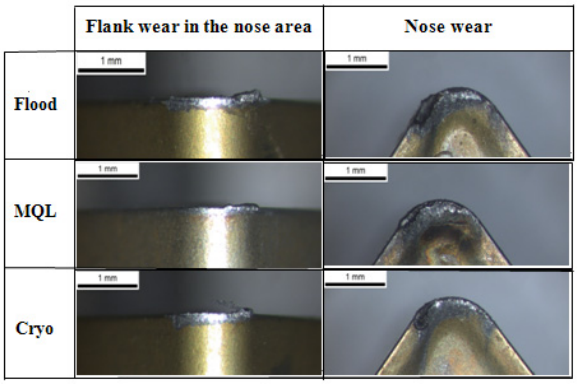

Fig. 2. Tool-wear images of machining *Ti-5553* alloy for flood-cooled, MQL and cryogenic conditions at cutting speed of 50 m/min and feed rate of 0.125 mm/rev.

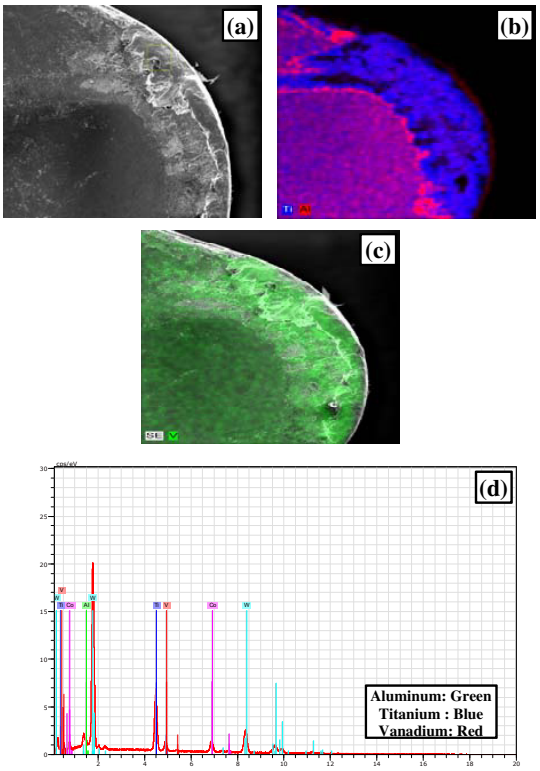

Fig. 3. The chemical elements distributed on the rake face of the insert: (a) SEM image showing the material adhesion on the rake face; (b) Titanium and aluminum distributions; (c) Vanadium distribution; (d) EDS analysis of different chemical compositions.

However, due to rapid cooling effect, the nose wear of the tool insert used in cryogenic machining was smaller compared with the other two tool inserts under flood-cooled and MQL conditions, while the amount of such nose wear in cryogenic machining is much smaller. The temperature in the cutting zone was reduced by the delivery of liquid nitrogen, and consequently there was less adhesion from the work material onto the insert rake face.

3.2. Forces

Two force components are presented in this paper, including cutting force parallel to the direction of cutting speed and thrust force perpendicular to the cutting speed direction. Three sets of the cutting and thrust forces were measured when the cutting speed was 50 m/min and the feed rate were 0.05, 0.125 and 0.2 mm/rev under the flood-cooled, MQL and cryogenic conditions. The comparisons among the three sets of forces are shown in Fig. 4. The cutting force from cryogenic machining were decreased by 6.3, 20.7 and 4.5%, respectively, compared to flood-cooled machining, while the decreasing percentage became 35.7, 7.1 and 32.4%, respectively, compared with MQL machining under the three different feed rates.

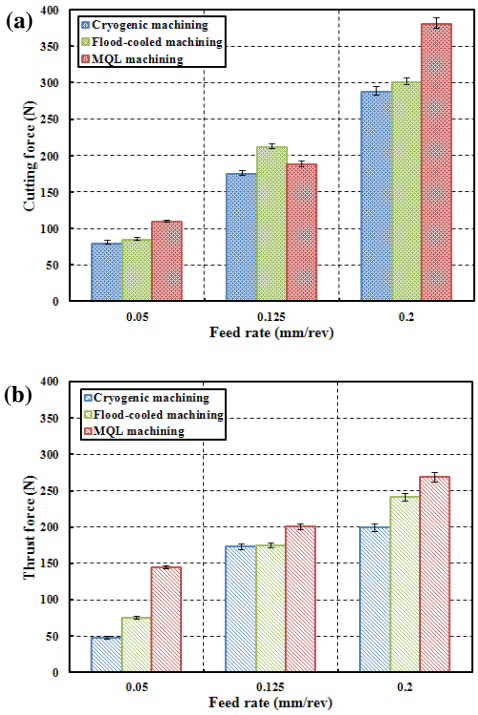

Fig. 4. Force comparisons among flood-cooled, MQL and cryogenic machining at the cutting speed of 50 m/min and the feed rates of 0.05, 0.125 and 0.2 mm/rev: (a) Cutting force; (b) Thrust force.

For the thrust force, 58.4, 1.1 and 21.2% reduction percentages were obtained in cryogenic machining compared to flood-cooled machining, while 203.5, 16.1 and 35.1% reduction percentages were achieved with the comparison with MQL machining, relating to the three feed rates,

respectively. A reasonable explanation for this is that less adhesion exists on the rake face of the tool inserts in the case of cryogenic machining as the liquid nitrogen lowered the temperature during machining, and in the meantime low friction took effect in the work material-tool and tool-chip contact areas. The highest force reductions occurred when the lowest feed rate was used due to smaller temperature elevation caused by less severe plastic deformation at a low feed rate and more effective cooling at a longer cutting time.

3.3. FEM model and simulation results

The commercial FEM software, DEFORM was used to perform the simulation of the numerical model. The *Ti-5553* work material was meshed with approximately 8000 isoparametric quadrilateral elements, while the tool insert was meshed with about 3000 elements. In the setup of the model, the work material was assumed to be visco-plastic, where the elastic part is neglected, and the tool insert was assumed rigid.

Fig. 5 shows the details of the model setup illustrating the thermal and velocity boundary conditions applied to the model. The cutting speed is applied horizontally on the bottom of the work material, and the bottom is fixed in the vertical direction. There is no specific velocity boundary condition used in left and right sides of the work material. For the purpose of analysing the thermal aspects, the top and right sides of the insert, as well as the bottom and left sides of the work material, are set to be at the room temperature. The heat exchange coefficient with the environment is set to be 20 W/(m^{2}K), which is the default value to simulate the free air convection. It is applied in the top and right sides of the work material, as well as the bottom and left sides of the tool insert.

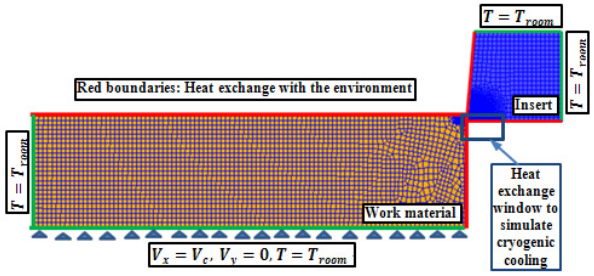

Fig. 5. Thermal and velocity boundary conditions applied to the FEM numerical model for cryogenic machining of *Ti-5553* alloy.

A heat exchange window is placed in the clearance side of the tool insert where the local temperature was set at -184 ºC, and the convection coefficient of the local heat exchange is 10000 kW/(m^{2}K) [25]. The shear friction model is used in the numerical model and the friction coefficient is fixed at 0.4 after certain calibrations. Johnson-Cook material model is modified and used as the flow stress model.

$$\sigma = \left(A + B\,\varepsilon^{n}\right)\left(1 + \mathrm{C}\ln\dot{\varepsilon}\right)\left[1 - \left(\frac{t - t_r}{t_m - t_r}\right)^{m}\right]$$

where σ represents the equivalent flow stress; ε and $\dot{\varepsilon}$ are the equivalent strain and effective strain-rate, respectively; constants A and B represent the initial yield strength and hardness modulus of the material; C is the strain-rate sensitivity coefficient; n and m represent the hardening coefficient and the thermal softening exponent; t, t_m and t_r are the temperatures of the workpiece, the material melting and the reference room, respectively. Based on the research of Özel et al. [26] and Germain et al. [27], the constitutive constants used in the model are as follows. The constant A and B are 1175 and 728 MPa, whereas the values of C, n, m, t_m and t_r are 0.09, 0.26, 0.72, 1630 ºC, 20 ºC, respectively. The mechanical properties for *Ti-5553* alloy are shown in Table 1.

Table 1. Properties of work material

Ti-5553 properties	
Young's Modulus (GPa)	110
Density (g/cm^3)	4.58
Poisson's ratio	0.31
Specific heat capacity (J/(kgK))	775
Melting temperature (K)	860
Elongation (%)	11

The cutting speed of 20 m/min and feed rates of 0.05, 0.125 and 0.2 mm/rev are selected to perform the simulation. Good agreements are achieved between the experimental data and simulated results for both the cutting and thrust forces, as shown in Fig. 6. Less than 7% difference was observed from the comparisons of cutting force, and less than 15% difference was found from the comparisons of thrust forces. Further modifications on the numerical model would be needed in the future to make more accurate simulation.

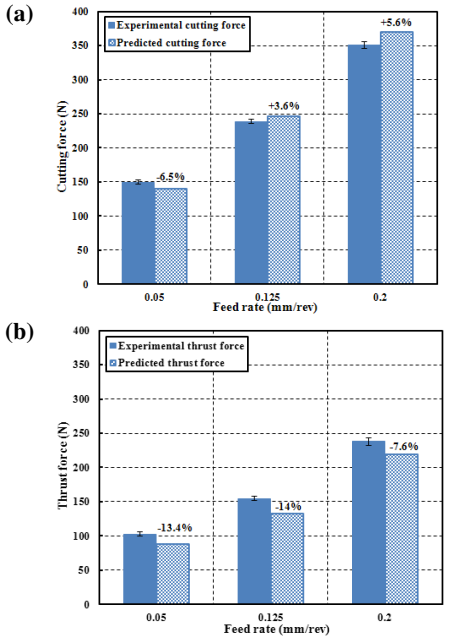

Fig. 6. The comparisons of experimental and predicted forces: (a) Cutting force; (b) Thrust force.

3.4. Surface roughness

Surface roughness of each machined sample from flood-cooled, MQL and cryogenic conditions are measured in five different areas, around the cylindrical surface across the feed marks. For each individual area, five lines were drawn on the

surface profiles and the surface roughness (R_a) values were measured, acquired and collected by the software associated with Zgyo NewView *5300* equipment. Fig. 7 illustrates the distributions of surface roughness at three different feed rates of 0.05, 0.125 and 0.2 mm/rev and the cutting speed of 50 m/min. The surface roughness increased with the increasing feet rates in all the three cooling conditions. The geometric expression shown by equation $R_a = f^2/(32R)$ would generally [28] explain the variation, where f represents the feed rate and R is the nose radius of the tool insert. However, this expression is not accurate for predicting the R_a at very low feeds [24]. Assuming that the nose radius is not changed because the cutting time is short and limited, an increased feed rate will result in a corresponding increase in the surface roughness at moderate to high feed rates. The effects of edge radius and the related size effects implicating the work-tool material interactions will play a role in machining at very low feed rates [29].

For low feed rates, the surface roughness measured on the sample from cryogenic machining is higher than that of flood-cooled and MQL machining. Higher temperature generated during machining of *Ti-5553* alloy provided the benefit to lower the surface roughness reported by Braham-Bouchnak et al. [23] and Baili et al. [15] in their study of laser assisted and hot machining. According to their study, higher ductility of the material would be prevalent at elevated temperatures. MQL machining used in this study is close to their cases, and this also provides some form of lubrication, thus reducing the frictional effects on the machined surface, particularly at larger feed rates. The surface roughness obtained from MQL machining is therefore smaller compared with the values for cryogenic and flood-cooled machining as more material would flow into the feed cavities caused by the insert nose due to higher ductility during MQL machining.

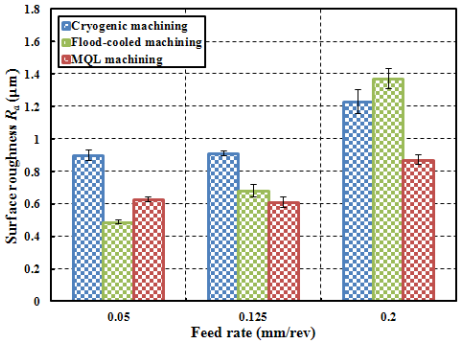

Fig. 7. Surface roughness comparisons of machined samples from cryogenic, flood-cooled and MQL conditions.

4. Conclusions

In this paper, liquid nitrogen has been used as the coolant during machining of *Ti-5553* alloy for the first time in the research community. The benefits of cryogenic machining of *Ti-5553* alloy were investigated by considering major machinability parameters such as tool-wear, forces and surface roughness. Cryogenic, flood-cooled and MQL machining of *Ti-5553* alloy were conducted in this study in which the cutting and thrust forces generated from cryogenic machining were reduced up to 30% compared with that of flood-cooled and MQL machining. Nose wear of the insert was improved in cryogenic machining due to reduced material adhesion. However, better surface roughness was observed in MQL machining due to high temperature and lubricity effects with the associated softening of the work material. The simulated and experimental cutting and thrust force components show good agreements. Predictions are made using the modified Johnson-Cook material equation in the FEM model. Further work proposed includes a study of surface integrity in cryogenic machining of *Ti5553* alloy.

References

[1] Jawahir IS, Brinksmeier E, M'Saoubi R, Aspinwall DK, Outeiro JC, Meyer D, Umbrello D, Jayal AD. Surface integrity in material removal processes: recent advances. CIRP Annals-Manufacturing Technology 2011; 60(2): 603-626.
[2] Kaynak Y, Tobe H, Noebe RD, Karaca HE, Jawahir IS. The effects of machining on the microstructure and transformation behavior of *NiTi* Alloy. Scripta Materialia 2014; 74: 60-63.
[3] Rotella G, Dillon Jr. OW, Umbrello D, Settineri L, Jawahir IS. The effects of cooling conditions on surface integrity in machining of *Ti6Al4V* alloy. Int J Adv Manuf Technol 2014; 71:47-55.
[4] Pu Z, Outeiro JC, Batistac AC, Dillon Jr. OW, Puleo DA, Jawahir IS. Surface integrity in dry and cryogenic machining of *AZ31B Mg* alloy with varying edge radius tools. Procedia Engineering 2011; 19: 282-287.
[5] Umbrello D, Micari F, Jawahir IS. The effects of cryogenic cooling on surface integrity in hard machining: A comparison with dry machining. CIRP Annals-Manufacturing Technology 2012; 61(1): 103-106.
[6] Pusavec F, Hamdi H, Kopac J, Jawahir IS. Surface integrity in cryogenic machining of nickel based alloy-Inconel 718. Journal of Materials Processing Technology 2011; 211: 773-783.
[7] Outeiro JC, Batista AC, Marques MJ. Residual stresses induced by dry and cryogenic cooling during machining of *AZ31B Mg* alloy. Advanced Materials Research 2014; 996: 658-663.
[8] Kaynak Y, Karaca HE, Noebe RD, Jawahir IS. Analysis of tool-wear and cutting force components in dry, preheated, and cryogenic machining of *NiTi* shape memory alloys. Procedia CIRP 2013; 8: 498-503.
[9] Kumar PM, Jerold DB. Effect of cryogenic cutting coolants on cutting forces and chip morphology in machining *Ti-6Al-4V* alloy. AIJSTPME 2013; 6(2): 1-7.
[10] Rotella G, Umbrello D. Numerical simulation of surface modification in dry and cryogenic machining of *AA7075* alloy. Procedia CIRP 2014; 12: 327-332.
[11] Kaynak Y, Karaca HE, Noebe RD, Jawahir IS. Tool wear analysis in cryogenic machining of *NiTi* shape memory alloys: A comparison of tool-wear performance with dry and MQL machining. Wear2013; 306: 51-63.
[12] Bermingham MJ, Palanisamy S, Kent D, Dargusch MS. A comparison of cryogenic and high pressure emulsion cooling technologies on tool life and chip morphology in *Ti-6Al-4V* cutting. Journal of Materials Processing Technology 2012; 212: 752-765.
[13] Pu Z, Outeiro JC, Batistac AC, Dillon Jr. OW, Puleo DA, Jawahir IS. Enhanced surface integrity of *AZ31B Mg* alloy by cryogenic machining towards improved functional performance of machined components. International Journal of Machine Tools & Manufacture 2012; 56:17–27.
[14] Pu Z, Puleo DA, Dillon Jr. OW, Jawahir IS. Controlling the biodegradation rate of magnesium-based implants through surface nanocrystallization induced by cryogenic machining. Proceedings of Magnesium Technology 2010, TMS Annual Meeting, Seattle, WA, 2010.
[15] Baili M, Wagner V, Dessein G, Sallaberry J, Lallement D. An experimental investigation of hot machining with induction to improve *Ti-5553* machinability. Applied Mech and Materials 2011; 62: 67-76.
[16] Ugarte A, M'Saoubi R, Garay A, Arrazola PJ. Machining behaviour of *Ti-6Al-4V* and *Ti-5553* alloys in interrupted cutting with PVD coated cemented carbide. Procedia CIRP 2012; 1: 202-207.
[17] Wagner V, Baili M, Dessein G, Lallement D. Behaviour laws comparison for titanium alloys machining: Application to *Ti-5553*. Key Engineering Materials 2010; 446: 147-155.
[18] Veeck S, Lee D, Boyer RR, Briggs RD. The microstructure and properties of cast titanium alloy *Ti-5553* were evaluated in a joint

program by Howmet and Boeing. Advanced Materials & Processes 2004; October: 47-49.
[19] Boyer RR, Briggs RD. The Use of β Titanium Alloys in the Aerospace Industry. JMEPEG 2005; 14:681-685.
[20] Bartus SD. Evaluation of Titanium-*5Al-5Mo-5V-3Cr (Ti-5553)* alloy against fragment and armor-piercing projectiles. ARL-TR-4996 September 2009.
[21] Arrazola PJ, Garay A, Iriarte LM, Armendia M, Marya S, Le Maitre F. Machinability of titanium alloys (*Ti6Al4V* and *Ti555.3*). Journals of Materials Processing Technology 2009; 209: 2223-2230.
[22] Wagner V, Baili M, Dessein G, Lallement D. Experimental study of coated carbide tools behavior: application for *Ti-5-5-5-3* turning. International Journal of Machining and Machinability of Materials 2011; 9: 233-248.
[23] Braham-Bouchnak T, Germain G, Morel A, Lebrun JL. The influence of laser assistance on the machinability of the titanium alloy *Ti555-3*. International Journal of Advanced Manufacturing Technology 2013; 68: 2471-2481.
[24] Shaw MC. Metal Cutting Principles. Oxford Series on Advanced Manufacturing, 2nd edition, Oxford University Press, USA, New York, 2005.
[25] Yang S. Cryogenic burnishing of *Co-Cr-Mo* biomedical alloy for enhanced surface integrity and improved wear performance. Doctoral Dissertation, University of Kentucky, 2012.
[26] Özel T, Zeren E. A methodology to determine work material flow stress and tool-chip interfacial friction properties by using analysis of machining. Journal of Manufacturing Science and Engineering 2006; 128: 119-129.
[27] Germain G, Morel A, Braham-Bouchnak T. Identification of material constitutive laws representative of machining conditions for two titanium alloys: *Ti6Al4V* and *Ti555-3*. Journal of Engineering Materials and Technology 2013; 135: 031002-1- 031002-11.
[28] Schey JA. Introduction of manufacturing processes (third edition). McGraw-Hill Series in Mechanical Engineering and Materials Science.
[29] Vollertsen F, Biermann D, Hansen HN, Jawahir IS, Kuzman K. Size effects in manufacturing of metallic components: CIRP Annals-Manufacturing Technology 2009; 58(2): 566-587.